to prepare the cell for repetitive secretion, are less vital for a neuroendocrine cell than for a synaptic terminal and thus proceed at different rates in the two types of cell. □

Received 6 October; accepted 10 December 1993.

1. Ishida, A. T., Stell, W. K. & Lightfoot, D. O. *J. comp. Neurol.* **191,** 315–355 (1980).
2. Sherry, D. M. & Yazulla, S. *J. comp. Neurol.* **329,** 188–200 (1993).
3. Kaneko, A. & Tachibana, M. *J. Physiol., Lond.* **358,** 131–152 (1985).
4. Heidelberger, R. & Matthews, G. *J. Physiol., Lond.* **447,** 235–256 (1992).
5. Marc, R. E. in *Neurobiology of the Inner Retina* NATO ASI (eds Weiler, R. & Osborne, N. N.) Series Vol. H31 53–64 (Springer, Berlin, 1989).
6. Heuser, J. E. & Reese, T. S. *J. Cell Biol.* **88,** 564–580 (1981).
7. Betz, W. J., Mao, F. & Bewick, G. S. *J. Neurosci.* **12,** 363–375 (1992).
8. Adler, E. N., Augustine, G. J., Duffy, S. N. & Charlton, M. P. *J. Neurosci.* **11,** 1496–1507 (1991).
9. Simon, S. M. & Llinás, R. R. *Biophys. J.* **48,** 485–498 (1985).
10. Zucker, R. S. & Fogelson, A. L. *Proc. natn. Acad. Sci. U.S.A.* **83,** 3032–3036 (1986).
11. Stern, M. D. *Cell Calcium* **13,** 183–192 (1992).
12. Raju, B., Murphy, B., Levy, L. A., Hall, R. D. & London, R. E. *Am. J. Physiol.* **256,** C540–C548 (1989).
13. Augustine, G. J. & Neher, E. *J. Physiol., Lond.* **450,** 247–271 (1992).
14. Tachibana, M., Okada, T., Arimura, T., Kobayashi, K. & Piccolino, M. *J. Neurosci.* **13,** 2898–2909 (1993).
15. Lindau, M. & Neher, E. *Pflügers Arch.* **411,** 137–146 (1988).
16. Jaffe, L. A., Hagiwara, S. & Kado, R. T. *Devl Biol.* **67,** 243–248 (1978).
17. Neher, E. & Marty, A. *Proc. natn. Acad. Sci. U.S.A.* **79,** 6712–6716 (1982).
18. Neher, E. & Zucker, R. S. *Neuron* **10,** 21–30 (1993).
19. Fernandez, J. M., Neher, E. & Gomperts, B. D. *Nature* **312,** 453–455 (1984).
20. Fidler Lim, N., Nowycky, M. C. & Bookman, R. J. *Nature* **344,** 449–451 (1990).
21. Lindau, M., Stuenkel, E. L. & Nordmann, J. J. *Biophys. J.* **61,** 19–30 (1992).
22. Thomas, P., Suprenant, A. & Almers, W. *Neuron* **5,** 723–733 (1990).
23. Thomas, P., Wong, J. G. & Almers, W. *EMBO J.* **12,** 303–306 (1993).
24. Del Castillo, J. & Katz, B. *J. Physiol., Lond.* **124,** 553–559 (1954).
25. Kandel, E. R. in *Principles of Neural Science* 3rd edn (eds Kandel, E. R., Schwartz, J. H. & Jessel, T. M.) 200–201 (Elsevier, New York, 1991).
26. Tachibana, M. & Okada, T. *J. Neurosci.* **11,** 2199–2208 (1991).
27. Verhage, M. *et al. Neuron* **6,** 517–524 (1991).
28. Maycox, P. R., Link, E., Reetz, A., Morris, S. A. & Jahn, R. *J. Cell Biol.* **118,** 1379–1388 (1992).
29. Kelly, R. B. *Neuron* **10** (Suppl.), 43–54 (1993).
30. Ryan, T. A. *et al. Neuron* **11,** 713–724 (1993).

ACKNOWLEDGEMENTS. We thank P. Brehm for comments on the manuscript and S. Yazulla for advice on goldfish retina. Supported by research grants from the NIH (G.M.) and by a NRSA postdoctoral fellowship (H.v.G.).

Localization of the site of Ca^{2+} release at the level of a single sarcomere in skeletal muscle fibres

Ariel L. Escobar*, Jonathan R. Monck†, Julio M. Fernandez† & Julio L. Vergara*‡

* Department of Physiology, University of California at Los Angeles, Los Angeles, California 90024, USA
† Department of Physiology and Biophysics, Mayo Clinic, Rochester, Minnesota 55905, USA

THE development of mechanical force in skeletal muscle fibres is brought about by rapid increases in the intracellular calcium concentration (Ca^{2+} transients) which can be detected by optical methods[1–7]. Local stimulation experiments[8] and ultrastructural evidence[9,10] suggest that, at a microscopic level, these Ca^{2+} transients are generated by the release of Ca^{2+} ions from the terminal cisternae of the sarcoplasmic reticulum in response to the depolarization of the transverse tubules (t-tubules)[11–14]. Nevertheless, to date, there is no functional information on the exact location at which Ca^{2+} release takes place. The present experiments were designed to obtain direct evidence about dynamic changes in localization and microscopic distribution of Ca^{2+} in a single sarcomere using two independent novel methodologies: confocal spot detection of Ca^{2+} transients[15,16] and Ca^{2+} imaging with pulsed laser excitation[17,18].

‡ To whom correspondence should be addressed.

TABLE 1 Properties of cgreen-5N and rhod-2 fluorescence signals detected at the Z- and M-lines in skeletal muscle fibres

Ca^{2+} dye	$(\Delta F/F)_Z$	$(\Delta F/F)_M$	$(t_{1/2})_Z$ (ms)	$(t_{1/2})_M$ (ms)
cgreen-5N	1.68 ± 9.42 (22)	1.39 ± 0.33 (22)	1.42 ± 0.19 (22)	3.51 ± 0.52 (20)
rhod-2	14.4 ± 9.6 (25)	8.7 ± 5.2 (8)	1.71 ± 0.31 (31)	3.55 ± 0.62 (14)

$(\Delta F/f)_Z$ and $(\Delta F/F)_M$ are the normalized peak amplitudes, and $(t_{1/2})_Z$ and $(t^{1/2})_M$ are the half-times, at the Z-line and centre of the sarcomere, respectively. The values of $(t_{1/2})_Z$ obtained with rhod-2 are significantly different from those obtained with cgreen-5N ($P < 0.0004$). In contrast, M-line transients with both dyes have almost identical $(t_{1/2})_M$ values ($P > 0.8$). Values are mean ± s.d. (number of observations).

Figure 1 shows Ca^{2+} transients recorded at different locations of a single sarcomere. Figure 1*a–c* shows the t-tubules lying in fine columns of increased fluorescence (black arrows) as revealed using a fluorescent potentiometric dye. Note that two columns of t-tubules define the boundaries of a sarcomere and, at the same time, serve as reference for the positioning of a fine spot of laser illumination (white arrows). The traces in Fig. 1*a–c* were obtained immediately before the muscle fibre was stimulated to generate action potentials; these in turn generated the fluorescence transients displayed in Fig. 1*d–f*. Whereas the fluorescence (Ca^{2+}) transients shown in Fig. 1*d* and *f* were recorded close to a t-tubule (see Fig. 1 *a* and *c*), the transient in Fig. 1*e* was obtained from the middle of the sarcomere (see Fig. 1*b*). In frog skeletal muscle, the t-tubules lie close to the Z-line[19], and the M-line of the contractile proteins lies at the centre of the sarcomere. Consequently, we will call signals detected close (within 0.5 μm) to the t-tubules 'Z-line transients' and those recorded at the centre of the sarcomere 'M-line transients'. Figure 1 shows that there are significant kinetic differences between Z-line and M-line transients. Note also that the $[Ca^{2+}]$ is only temporarily elevated through the sarcomere, as both Z- and M-line transients eventually return to baseline.

Figure 2 compares the kinetic features of Ca^{2+} transients detected at the two locations in a more expanded timescale. Superimposed Z- and M-line traces obtained in fibres stained with the Ca^{2+} dyes cgreen-5N (ref. 20) and rhod-2 (refs 12, 13, 21) are shown in Fig. 2*a* and *b*, respectively. There is an identical time delay of about 3 ms before the onset of every fluorescence transient, irrespective of the location of the recording spot and the Ca^{2+} due used. In addition, after this constant delay, the rising phases of Z-line transients are always faster than those of M-line transients. However, Z-line transients recorded with cgreen-5N display faster-rising kinetics than those recorded at the same location with rhod-2 (Table 1). The large difference in the dissociation constants (K_ds) of cgreen-5N[20] and rhod-2[13,21] (see Fig. 2 legend) may account for this difference. In contrast, M-line transients recorded with both dyes show similar, but slower, kinetics (Table 1). Together, these comparisons demonstrate that localized transients have significant location-dependent kinetic characteristics and few dye-dependent differences, in spite of the large differences in the dye properties.

Table 1 compares the amplitudes and kinetic properties of confocal records obtained from 11 single-fibre experiments. It is clear that, despite large differences in the amplitude of the fluorescence transients detected with each Ca^{2+} dye, the rising half-times ($t_{1/2}$) depend mostly on the location of the spot in the sarcomere. Thus, $(t_{1/2})_Z$ values recorded with both Ca^{2+} dyes are significantly shorter than $(t_{1/2})_M$ values ($P < 0.00001$). These findings strongly suggest proximity to the release site in the case of the Z-line transients and a more remote site for the M-line transients. Interestingly, however, there is no significant extra delay in the onset of the M-line transients, as would be expected

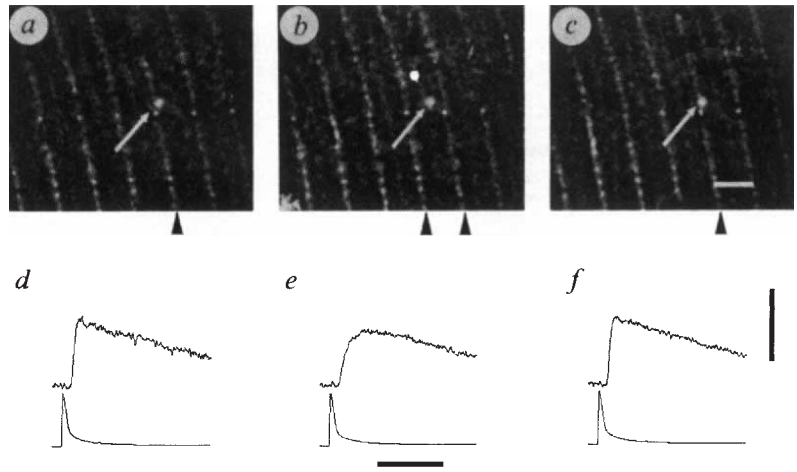

FIG. 1 Confocal spot detection of intra-sarcomeric Ca^{2+} transients. A laser beam was focused into minute areas of a frog skeletal muscle fibre stained intracellularly with 500 μM of the Ca^{2+} dye cgreen-5N[20]. They are displayed as fluorescence spots (white arrows) in the images shown in *a–c*. The position of the t-tubules was determined using the potentiometric dye RH-795 (ref. 28). They can be observed as fine columns of increased fluorescence (black arrows, *a–c*). The faint fluorescence in the middle of the sarcomere is caused by spectral overlap between cgreen-5N (homogeneously staining the sarcomeric volume) and RH-795. Scale bar in *c*, 4 μm. Changes in the epifluorescence of the Ca^{2+} dye at the spot, caused by electrical stimulation of the muscle fibre, were detected with a PIN photodiode (with a detection area of 0.008 mm^2) centred on the spot image (upper traces; *d–f*). Every fluorescence record is matched with its respective action potential (lower traces; *d–f*). Time calibration bar in *e*, 20 ms for traces in *d–f*. The vertical bar in *f* gives $\Delta F/F$ and membrane potential calibrations of 2 and 150 mV, respectively.

METHODS. An inverted double Vaseline gap chamber[14] was used for simultaneous recording of high-magnification images, electrical activity and localized detection of fluorescence transients in single skeletal muscle fibres dissected from the semitendinosus muscle of the bullfrog *Rana catesbeiana*. The cut ends of the fibres were bathed in an internal solution containing: 110 mM K–maspartate; 20 mM K-MOPS; 5 mM sodium phosphocreatine, 5 mM Na_2–ATP, 150 μM EGTA, 3 mM $MgCl_2$, 0.1 mg ml^{-1} creatine kinase, pH 7.0, 245 mosmols. The Ca^{2+} dyes rhod-2 and cgreen-5N were added to the internal solution at the concentrations indicated in each experiment. To prevent movement, the muscle fibres were stretched to a sarcomere spacing of 3.8–4.0 μm. They were externally perfused in the central pool with Ringer's solution at 15 °C and also stained extracellularly with 10 μM of the potentiometric dye RH-795. The chamber was palced on the stage of an inverted fluorescence microscope (Zeiss) modified for confocal spot detection, and a Nikon Fluo100 (NA 1.3) objective was used to form the image of the muscle fibre. A xenon lamp provided whole-field epillumination for the dye RH-795 ($\lambda_{excitation}$: 570 nm; $\lambda_{emission}$: 640 nm The raw images were obtained with a cooled CCD camera (MCD220; Spectra Source, Agoura Hills, California) and deblurred[29] to yield the images displayed in *a–c*. An argon laser (Model 80; Lexel, California) was focused to illuminate a 0.5-μm spot of the fibre. The local Ca^{2+} transients were detected by a PIN photodiode connected to a patch-clamp amplifier with 50 GΩ feedback (Axon Instruments, CV-1A, Foster City, California). The depth of field[30] of the spot confocal detection system was measured as 1.1 μm. The optical analog signals were acquired, simultaneously with the membrane voltage, by a data acquisition system (Axon Instruments). The fluorescence before stimulation of the muscle fibres was used to calculate the $\Delta F/F$ values. Potentiometric and Ca^{2+} dyes were obtained from Molecular Probes (Eugene, Oregon).

from the diffusional distance (~2 μm) separating the two detection spots.

To investigate whether these kinetic differences result in $[Ca^{2+}]$ gradients detectable in register with sarcomeric structures, we performed experiments using a pulsed laser imaging setup[18]. 'Snapshot' images obtained at short times after stimulation (for example, 4 ms; Fig. 3*b*) show a massive increase in Ca^{2+}-dependent fluorescence compared with the fluorescence of the resting muscle fibre. The image in Fig. 3*b* also reflects large inhomogeneities in the distribution of Ca^{2+} in the sarcomere, not seen in Fig. 3*a*. The high-fluorescence bands show the same periodicity as sarcomeric structures visualized with bright-field illumination (Fig. 3*d*). Moreover, it is clear that the banded appearance in the fluorescence snapshot images disappears 10 ms after stimulation

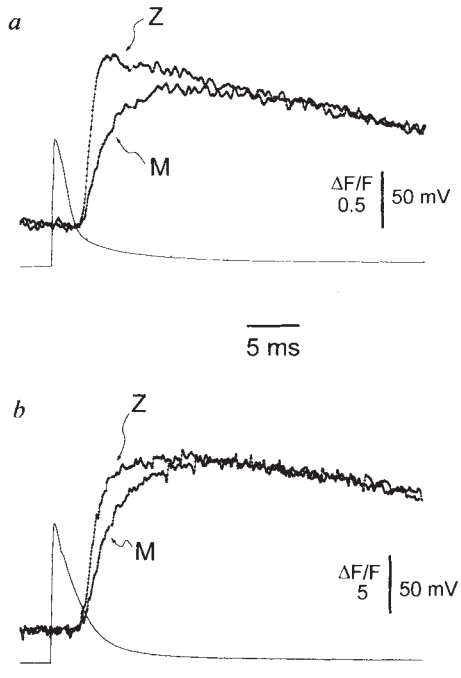

FIG. 2 *a*, Superposition of Z- and M-line transients (traces Z and M, respectively) elicited by action potentials (lower trace) recorded from a fibre stained with 500 μM cgreen-5N. The two single sweep traces were recorded consecutively at alternate positions of the spot, ensuring that the kinetic differences were dependent only on the spot position in the sarcomere and not on the order of sampling. *b*, Records obtained from a similar experiment using 300 μM rhod-2. The K_d values, obtained by fitting cuvette data to a saturation formula[13], were 45 μM and 1.3 μM for cgreen-5N and rhod-2, respectively. The ratio between maximal to minimal fluorescence (F_{max}/F_{min}) was 10 for cgreen-5N and 143 for rhod-2.

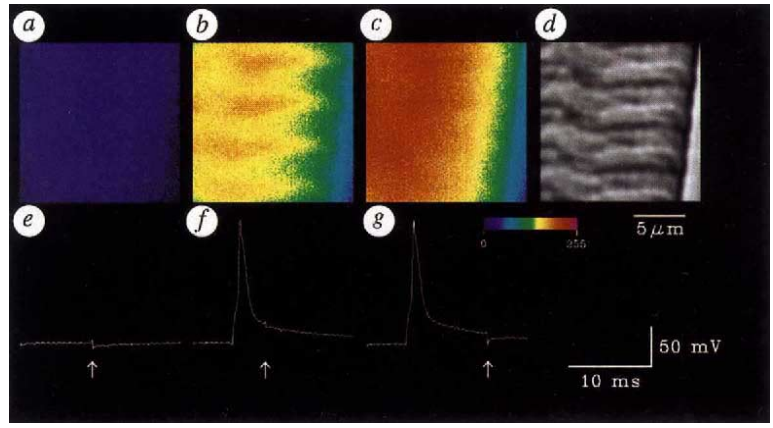

FIG. 3 *a–c*, A sequence of pulsed laser ('snapshot') fluorescence images of a muscle fibre stained intracellularly with 300 μM rhod-2. They were obtained by delivering a 300-ns flash to the muscle fibre at rest, and 4 ms and 10 ms after stimulation (*a*, *b* and *c*, respectively). The analog traces in panels *e–g* are records of the action potentials and show the flash delivery artefact. The colour bar shows the arbitrary pseudo-colour rendering of the fluorescence intensity for a linear scale from 0 to 256. *d* was obtained before electrical stimulation using bright-field illumination. The dye laser was triggered with different delays with respect to the electrical stimulation of the fibre (white arrows).

METHODS. A single muscle fibre was mounted using the procedure described in Fig. 1 legend. The recording chamber was placed instead on an optical sectioning microscope[18,29] equipped with a high-intensity (480 mJ at 560 nm) pulsed coaxial flash lamp dye laser (Model LS-1400, Luminex; 300 ns flash duration). A light guide coupled the laser to the epifluorescence port of the microscope, where a lens focused the light so as to illuminate the entire field of view. A Nikon 100 × (NA 1.3) objective was used to view the muscle fibre.

(Fig. 3*c*) whereas the overall fluorescence is still largely increased. The fluorescence images in Fig. 3 give an independent 'visualization', in a two-dimensional view, of the results presented in Figs 1 and 2. Namely, snapshot detection of the fluorescence image 4 ms after stimulation indicates a fluorescence pattern in which the high intensities must be centred on the Z-lines. In contrast, the snapshot image at 10 ms suggests that throughout the sarcomere there is homogeneously high $[Ca^{2+}]$. An additional point of agreement between the Ca^{2+} distribution reported in the snapshot images and the kinetic properties of the fluorescence records is that at 4 ms, although the fluorescence is higher at the Z-line than at the centre of the sarcomere, in the latter region it is significantly higher than the basal level.

Our results provide the first direct experimental support for the hypothesis that, in skeletal muscle fibres, the primary Ca^{2+}-release sites are located at the terminal cisternae of the sarcoplasmic reticulum. The detection of out-of-focus information[22] limits our ability to distinguish between kinetic events occurring in close proximity. Nevertheless, this limitation cannot readily explain why M- and Z-line transients may share a common origin (with no extra lag) and very different kinetics. Instead, our results suggest the interesting possibility that a broad band of sarcoplasmic reticulum may participate in the release process; this possibility is supported by the presence of extra-junctional Ca^{2+}-release channels in skeletal muscle[23]. Finally, the present experiments describe new methodologies that are ideal for locating sites of fast Ca^{2+} release in any biological preparation, providing an alternative technique when other imaging methods[6,24–27] fail. □

Received 23 September; accepted 16 December 1993.

1. Ebashi, S. & Endo, M. *Prog. Biophys. molec. Biol.* **18,** 123–183 (1968).
2. Sandow, A. *A. Rev. Physiol.* **32,** 87–138 (1970).
3. Miledi, R., Parker, S. & Schalow, G. *Prog. R. Soc.* B**198,** 201–211 (1977).
4. Palade, P. & Vergara, J. *J. gen. Physiol.* **79,** 679–707 (1982).
5. Baylor, S. M., Chandler, W. K. & Marshall, M. *J. Physiol., Lond.* **331,** 179–210 (1982).
6. Vergara, J., Di Franco, M., Compagnon, D. & Suarez-Isla, B. *Biophys. J.* **59,** 12–24 (1991).
7. Vergara, J. & DiFranco, M. *Adv. Exp. Med. Biol.* **311,** 227–236 (1992).
8. Huxley, A. F. & Taylor, R. E. *J. Physiol., Lond.* **144,** 426–441 (1958).
9. Winegrad, S. *J. gen. Physiol.* **55,** 77–88 (1970).
10. Somlyo, A. V. *et al. J. Cell Biol.* **90,** 577–594 (1981).
11. Endo, M. *Physiol. Rev.* **57,** 71–108 (1977).
12. Schneider, M. F. & Chandler, W. K. *Nature* **242,** 244–246 (1973).
13. Rios, E. & Pizarro, G. *Physiol. Rev.* **71,** 849–908 (1991).
14. Fleisher, S. & Inui, M. *A. Rev. Biophys. biophys. Chem* **18,** 333–364 (1989).
15. Escobar, A. & Vergara, J. *Biophys. J.* **64,** A241 (1993).
16. Parker, I. & Ivorra, I. *J. Physiol., Lond.* **461,** 133–165 (1992).
17. Hibino, M., Sigemori, M., Itoh, H., Nagayama, K. & Kinosita, K. Jr, *Biophys. J.* **59,** 209–220 (1991).
18. Monck, J. R., Escobar, A., Robinson, I. M., Vergara, J. & Fernandez, J. M. *Biophys. J.* **66,** A351 (1994).
19. Peachey, L. D. *J. Cell Biol.* **25,** 209–231 (1965).
20. Vergara, J. & Escobar, A. *Biophys. J.* **64,** A37 (1993).
21. Minta, A. *et al. J. biol. Chem.* **264,** 8171–8178 (1989).
22. Wilson, T. & Carlini, A. R. *Opt. Lett.* **12,** 227–229 (1987).
23. Dulhunty, A., Junankar, P. & Stanhope, C. *Proc. R. Soc.* B**247,** 69–75 (1992).
24. Takamatsu, T. & Wier, W. G. *Cell Calcium* **11,** 111–120 (1990).
25. Niggli, E. & Lederer, W. J. Cell Calcium **11,** 121–1130 (1990).
26. Parker, I. & Yao, Y. *Proc. R. Soc.* B**246,** 269–274 (1991).
27. Girard, S. & Clapham, D. *Science* **260,** 229–232 (1993).
28. Grinvald, A., Frostig, R., Lieck, E. & Hildesheim, R. *Physiol. Rev.* **68,** 1285–1358 (1988).
29. Monck, J., Oberhauser, A., Keating, T. & Fernandez, J. *J. Cell Biol.* **116,** 745–759 (1992).
30. Sheppard, J. R. *J. Microsc.* **149,** 73–75 (1998).

ACKNOWLEDGEMENTS. We thank S. Krasne and P. Verdugo for reading a previous version of the manuscript, J.Kidokoro for the loan of the Argon laser, J. Ribas for help with some confocal spot detection experiments and C. Perez for help with the pulsed laser imaging experiments. This work was supported by grants from the NIH (J.L.V., J.M.F.) and the MDA (J.L.V.).

Terminal pattern elements in *Drosophila* embryo induced by the *torso-like* protein

Jean-René Martin, Anna Raibaud & Roger Ollo

Institut Pasteur, Laboratoire de Biologie Moléculaire de la Drosophile, 25, rue du Docteur Roux, 75724 Paris, cedex 15, France

THE genes *torso* (*tor*)[1] and *torso-like* (*tsl*)[2] are two of the *Drosophila* maternal group genes implicated in a receptor tyrosine kinase signalling pathway that specifies terminal cell fate (reviewed in ref. 3). Loss-of-function mutations in these loci cause an identical phenotype in which pattern elements from the anterior (acron) and posterior (telson) ends have been deleted. We have cloned the *tsl* gene and demonstrate here that, in agreement with previous genetic data, it encodes a protein that is secreted and whose transcription is restricted to specialized categories of follicle cells localized at the poles of the egg chamber. At early blastoderm stage, *tsl* protein forms a symmetrical concentration gradient at the poles on the surface of the devitellinized embryo. Unrestricted expression of the *tsl* protein in *tsl* female mutants induces terminal pattern elements and suppresses the formation of abdomen in embryos. These results suggest that the *tsl* protein is the ligand that binds to the *torso* receptor.

The *torso* gene encodes a putative transmembrane protein that is similar to receptor tyrosine kinases[4]. The *torso* protein is expressed uniformly on the surface of all early embryonic cells, but is activated only at the poles of the embryo[5–7]. Consistent with the prediction of a spatially localized ligand in the receptor